

Depositional environments of “accreted bedded cherts” in the Shimanto terrane, Southwest Japan, on the basis of major and minor element compositions

Koshi YAMAMOTO*, Kango NAKAMARU and Mamoru ADACHI***

**Department of Earth and Planetary Sciences, Graduate School of Science,
Nagoya University, Nagoya 464-01, Japan*

***The Shin-Nippon Meteorological & Oceanographical
Consultants CO., LTD., Nishi, Osaka 550, Japan*

(Received June 20, 1997 / Accepted July 31, 1997)

ABSTRACT

Chemical characteristics and depositional environments of bedded cherts collected from a melange block in the Cretaceous northern Shimanto terrane were examined on the basis of their major and minor element compositions. The bedded cherts, accompanied by underlying pillow basalts, have been considered to be a part of an “accretional prism” originated in a low-latitude ocean ridge region far from the present position. However, geochemical data show that the bedded cherts are not enriched in hydrothermal elements such as Fe and Mn, and have deposited in an environment free from intense hydrothermal activities usually found around an ocean ridge. The present data, as well as those of marine sediments from various environments, demonstrate that the so-called “accreted bedded cherts” in the Shimanto terrane are not deep pelagic in origin but formed in a hemipelagic environment such as offshore or marginal sea.

INTRODUCTION

The pre-Neogene basement of Southwest Japan comprises several terranes arranged parallel to the trench axis of the Nankai trough. The origin and depositional environment of bedded cherts in the basement are still controversial. Bedded cherts in the Cretaceous to Paleogene Shimanto terrane that occupies the southernmost part of these terranes have been paleo-magnetically studied. Kodama et al. (1983) and Hirooka et al. (1983) reported that the remanent magnetization of basaltic rocks and red sediments from the terrane shows significantly shallow inclinations and scattered declinations after correction for tilt of the strata. They claimed, on the basis of the shallow inclinations, that the basaltic rocks and red sediments in the Shimanto terrane originated in low-latitude areas far from the present position of the Japanese Islands and were accreted to the Japanese Island Arc. They also explained the scattered declinations by the disarrangement of each allochthonous body at the time of the accretion into the subduction complex. On the other hand, Hayashida et al. (1988) pointed out that some Shimanto allochthonous bodies

might have been subjected to secondary overprint in the subduction complex. Shibuya and Sasajima (1986) showed that Jurassic red cherts in the Mino terrane, central Japan, have the secondary magnetic overprint carried by titanomagnetite. If this is the case, the significantly shallow inclinations reported by Kodama et al. (1983) and Hirooka et al. (1983) are not intrinsic and the erupting and sedimentary environments of basaltic and sedimentary rocks, respectively, are not necessarily pelagic and cannot be deduced from the paleomagnetic data up to date.

We approach to the problem on the basis of chemical properties intrinsic to those materials. Silica-rich radiolarian ooze occurs widely in the low-latitude high-productivity regions. By analogy, bedded cherts have been believed to originate in such regions. As an example of the case, Yamamoto (1987) and Murray et al. (1990, 1991) have geochemically examined bedded cherts in the Franciscan terrane, Pacific coast of North-America, and concluded that stratigraphically lower-horizon bedded cherts were deposited in an ocean-ridge region far from the present position. In contrast, geochemical data showing a non-pelagic origin of bedded cherts have been obtained from the bedded cherts in the Mino terrane, central Japan; including rare earth element compositions (Shimizu and Masuda, 1977), major and trace element compositions (Sugisaki et al., 1982; Yamamoto, 1983), Ce-Nd isotopic systematics (Shimizu et al., 1991) and chemical compositions of manganese carbonate band and manganese micro-nodules associated with the cherts (Sugisaki et al., 1987, 1991). All these authors concluded that the bedded cherts had deposited in the hemipelagic environment such as continental slope or marginal sea.

Siliceous sedimentary rocks, particularly chert, are more stable against weathering than other sedimentary rocks, and thus provide important information on their sedimentary environments. In this study, we have analyzed major and minor elements for cherts and shale partings in a bedded chert block in the Shimanto terrane, which is generally considered to be an "accretionary prism" that originated in a low-latitude ocean ridge region (Taira et al., 1980; 1985). The purposes of this study are (1) to describe the geochemical characteristics of so-called "accreted bedded cherts" in the Shimanto terrane, (2) to compare them to the bedded cherts from the Franciscan and the Mino Terrane that are considered geochemically to have been deposited in the ocean-ridge and hemipelagic regions, respectively, and (3) to deduce geochemically the depositional environment of "accreted bedded cherts".

SAMPLING LOCATION and SAMPLE DESCRIPTION

The Shimanto terrane is one of the major geologic units in the Southwest Japan. According to the previous studies (e.g. Taira et al., 1980), the Shimanto terrane is divided into Cretaceous Northern and Tertiary Southern belts separated by the Aki-Sukumo Tectonic Line.

Analyzed samples were collected from a melange block of bedded chert outcropping at Tei to the east of Kochi City, Shikoku, in the Cretaceous

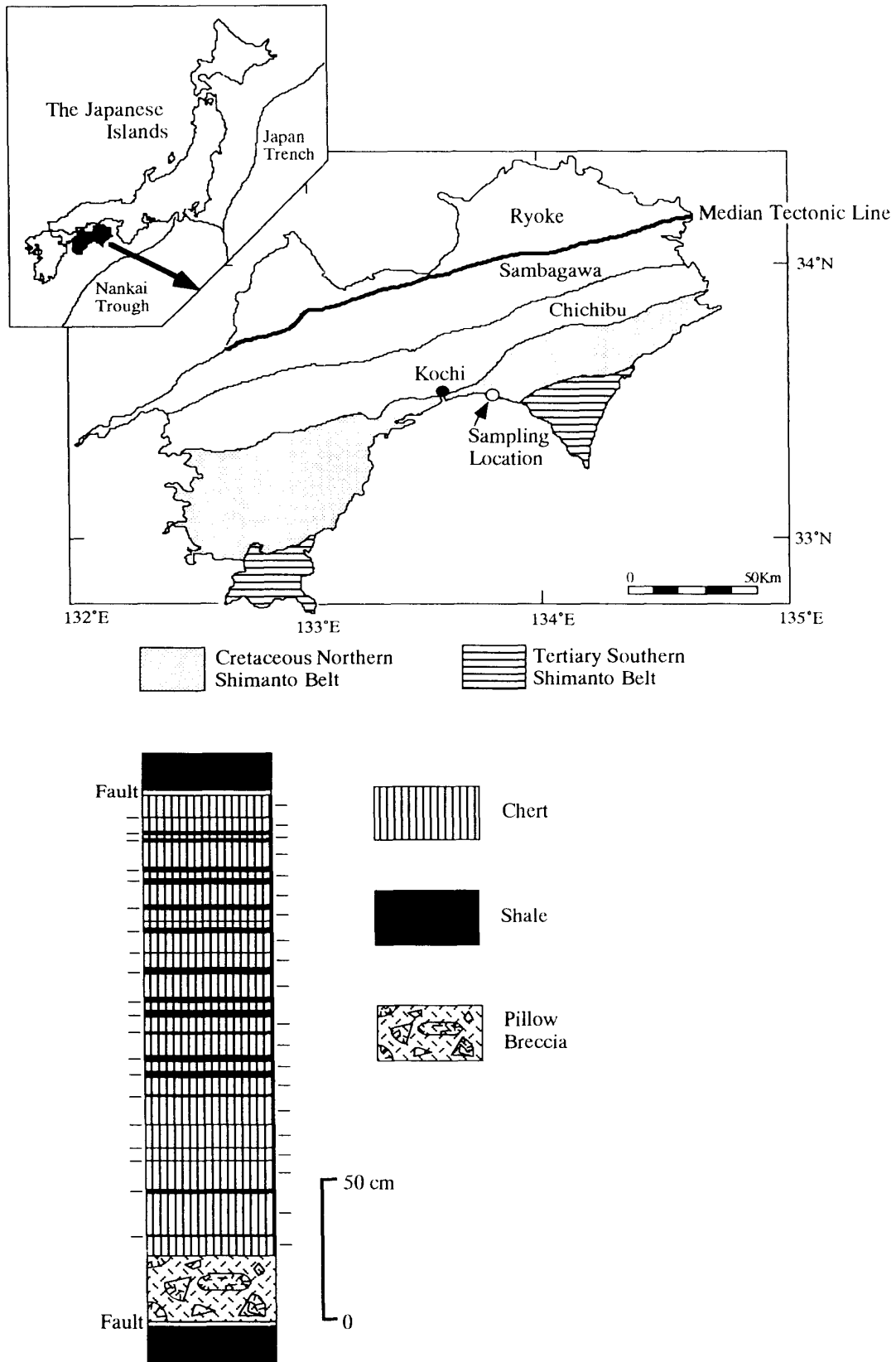


Fig. 1. Sampling location (open circle) and columnar section of the Shimanto bedded cherts in Shikoku. Horizontal bar on the right side of the columnar section indicates sampling horizon of chert, and that on the left side for shale.

Northern Shimanto belt (Fig. 1). Bedded cherts accompanied by underlying pillow breccia are entrained in tectonic melange as a block. Three underlying basalts, 22 cherts and 24 shale partings were collected from the melange block. The chert layers are reddish brown in color and 3 to 10 cm thick, and the shale layers are also reddish brown in color and about <1 cm thick. Early Cretaceous radiolarians have been reported from the Tei bedded cherts (Taira et al., 1980).

The basal pillow basalt consists of plagioclase with minor amounts of altered clinopyroxene and opaques such as hematite and shows well-developed variolitic texture. The chert is composed mainly of micro-crystalline quartz, clay minerals and radiolarian remains, with lesser amounts of opaque minerals. The chert is commonly cut by calcedonic quartz veins. The radiolarian tests are infilled usually with length-fast chalcedony and sometimes with chlorite or monocrystalline quartz. Angular detrital plagioclase and/or poikilitic basaltic fragments are disseminated parallel to the bedding in the lower horizon chert. The shale is composed of clay minerals, basaltic fragments, detrital plagioclase and opaque minerals, with minor amounts of radiolarian tests. Basaltic fragments with poikilitic texture and angular detrital plagioclase grains tend to be more abundantly disseminated in shales from the lower horizon. Observation by a JEOL JSM840A scanning electron microscope (SEM) equipped with a Link energy-dispersive analytical system (EDS) has shown that the titanium-bearing mineral sphene is ubiquitously contained in shales. The basaltic fragments in cherts and shales do not seem to have originated directly from the underlying pillow basalt, because their textures are completely different to each other.

ANALYTICAL METHOD

Samples were crushed into mm size with an iron mortar, then washed ultrasonically with distilled water and ground into <120 mesh with an agate mortar. Major and minor elements were analyzed on an automatic X-ray fluorescence spectrometer, Rigaku 3270E, at Kobe University. For the measurement of major elements, glass beads were prepared by fusing mixtures of 0.5 g sample with 5 g lithium tetraborate. The 2 g sample was mixed with 3 g panorack (Dai-Nihon Ink Co., LTD.) and pressed under 300 kg/cm² for preparation of pellets for the minor element analyses. Matrix effect of each sample was corrected for determination of major and minor elements. For the determination of Rb, Y, Zr and Nb, interferences of K β line of Br, Rb, Sr and Y to the former elements, respectively, were corrected. Analytical errors, estimated from measurements of standard rock samples published by Geological Survey of Japan, are less than 5% for major elements and less than 20% for minor elements. Ferrous iron and H₂O were determined by colorimetric and gravimetric method, respectively. No carbonate was detected for the present samples.

RESULTS and DISCUSSION

The analytical results are listed in Table 1. Some shale layers were too thin to collect enough quantity of sample for the minor element analysis. The chemical composition recalculated on a volatile-free basis may be more advantageous to discuss genetic relationship of cherts with shales because of the difference of volatile contents; almost all shales contain more than 3.5% H₂O, whereas cherts do less than 2% H₂O. Table 2 shows such a comparison of average compositions of the present samples with those from the Mino terrane, central Japan (Yamamoto, 1983) and the Franciscan terrane (Yamamoto, 1987).

Relationship between SiO₂ and other elements

As shown in Table 2, the Shimanto cherts contain lesser amounts of SiO₂ and larger amounts of TiO₂, Al₂O₃, MgO, Ga, Sr, Zr, etc. than the Mino and Franciscan cherts. This may be ascribed to the difference of dilution degree by biogenic silica mainly of radiolarian tests. To examine this, SiO₂ contents of the Shimanto, Mino and Franciscan samples are plotted against concentrations of TiO₂, Al₂O₃, total iron as Fe₂O₃ (hereafter "total Fe₂O₃") and Zr (Fig. 2). Sugisaki et al. (1982) and Yamamoto (1983) pointed out that the Mino cherts and shales cluster along a line in these diagrams and have correlation coefficients of SiO₂ vs. other elements less than -0.95. They explained the strong inverse correlations by different mixing degrees of biogenic silica with other elements of lithogenic origin in each sample. The Shimanto bedded cherts also define a line passing through the point of pure SiO₂. This also shows that mixing of biogenic silica with lithogenic materials is responsible for the formation of the Shimanto bedded cherts. Large amounts of radiolarian tests found in the Shimanto bedded cherts support the mixing processes. The depletion of SiO₂ and enrichment of TiO₂ and other elements of the Shimanto cherts in comparison with the Mino and Franciscan cherts are mainly due to the difference of dilution degree by biogenic silica.

For comparison among bedded cherts from the three areas, regression lines for the Mino bedded cherts were depicted in the figures of other area (Fig. 2). Shimanto cherts and shales are plotted above or below the regression line for the Mino bedded cherts in Fig. 2. This suggests that the composition of lithogenic materials contained in the Shimanto bedded cherts are different from that in the Mino bedded cherts; that is, lithogenic materials in the Shimanto bedded cherts are enriched in total Fe₂O₃ and depleted in Al₂O₃ and Zr in comparison with those in the Mino bedded cherts.

On the SiO₂-TiO₂ diagram (Fig. 2), the Shimanto cherts cluster along the regression line for the Mino bedded cherts, whereas the Shimanto shales are plotted in a wide field on the right side of the line. This implies that the lithogenic materials contained in cherts are different from those in the shales; clastic materials in the cherts have similar TiO₂ content with those in the Mino bedded cherts but clastics in the shales have higher TiO₂ content than

Table 1. Analytical results of cherts, shales, and basalts from the Shimanto terrane (oxides and residual materials are expressed in % and metals are in ppm).

Name	1	2	3	4	5	6	7	8	9	10	11	12	13	14	15	16
	Basalt	Basalt	Basalt	Shale	Shale	Shale	Chert	Shale	Chert	Shale	Chert	Shale	Chert	Shale	Chert	Shale
SiO ₂	46.52	45.49	47.46	51.66	59.99	52.78	88.22	53.57	85.05	60.21	75.10	51.39	84.42	56.07	92.56	53.57
TiO ₂	1.93	1.69	2.04	1.78	0.91	2.00	0.22	1.39	0.28	1.22	0.51	1.99	0.40	1.69	0.10	1.93
Al ₂ O ₃	16.97	14.56	17.25	16.87	13.57	18.27	4.00	16.70	5.54	13.70	9.53	14.86	5.37	14.77	2.53	15.50
FeO	2.85	2.08	2.52	1.23	1.05	1.38	1.00	0.74	1.59	1.00	0.86	0.84	1.05	0.84	0.99	0.74
Fe ₂ O ₃	8.75	9.38	7.55	10.21	9.50	8.17	1.83	8.57	1.65	7.65	3.76	11.20	3.08	8.81	1.22	8.23
MnO	0.19	0.18	0.24	0.18	0.14	0.12	0.09	0.16	0.10	0.17	0.13	0.20	0.11	0.17	0.06	0.13
MgO	5.93	4.79	6.50	2.73	2.23	1.69	1.33	2.95	1.42	2.78	1.67	2.64	1.44	2.02	0.63	1.67
CaO	7.41	9.90	3.48	3.94	2.02	4.83	0.56	2.32	1.12	2.16	1.95	3.94	0.76	3.63	0.29	4.44
Na ₂ O	3.92	4.24	2.69	5.78	3.32	4.91	0.85	2.55	1.42	2.27	2.16	2.85	0.87	4.33	0.41	6.26
K ₂ O	0.76	0.52	3.81	1.39	2.39	2.01	0.68	4.40	0.61	3.20	1.35	3.33	1.17	2.05	0.41	1.65
P ₂ O ₅	0.28	0.26	0.32	0.30	0.23	0.33	0.12	0.44	0.24	0.43	0.29	1.32	0.21	1.19	0.05	1.77
H ₂ O(-)	1.21	0.94	1.48	0.82	1.13	0.79	0.49	1.54	0.49	1.27	1.13	1.60	0.39	0.85	0.17	0.89
H ₂ O(+)	2.41	2.33	4.12	1.87	2.12	1.49	0.82	3.40	1.43	3.05	2.40	3.42	1.55	2.49	0.54	1.82
Res.	0.24	3.93	0.25	0.28	0.12	0.20	0.56	0.12	0.24	0.00	0.10	0.06	0.23	0.48	0.52	0.58
Co	54	42	46	45	31	25	12	24	15	27	18		17		9	
Ni	480	180	100	110	60	67	30	62	34	61	46		42		23	
Cu	13	15	76	34	18	91	22	67	17	35	32		49		57	
Zn	140	120	140	140	120	110	60	130	69	130	93		87		41	
Ga	24	18	23	20	19	19	8	25	7	22	13		11		5	
Rb	8	4	87	30	67	49	20	120	15	97	37		34		9	
Sr	310	280	200	400	320	40	55	190	89	160	130		58		36	
Y	32	26	37	33	36	42	17	48	23	40	31		26		10	
Zr	150	130	170	140	140	150	41	240	60	170	90		65		17	
Nb	19	18	21	18	10	20	6	15	7	12	8		8		5	
Pb	2	0	3	3	8	15	2	8	1	17	6		5		3	
Th	6	5	3	3	6	3	4	9	5	10	5		6		4	
Ba	240	250	430	300	320	290	69	370	95	420	190		160		57	
Name	17	18	19	20	21	22	23	24	25	26	27	27'	28	29	30	31
	Chert	Shale	Chert	Shale	Chert	Shale	Chert	Shale	Chert	Shale	Chert	Shale	Shale	Chert	Chert	Shale
SiO ₂	95.11	50.66	91.22	50.39	82.30	52.31	73.91	63.52	89.18	52.47	87.60	59.27	56.22	82.51	96.62	55.29
TiO ₂	0.08	1.39	0.15	1.31	0.22	1.38	1.58	1.89	0.15	1.22	0.22	1.11	1.12	0.36	0.05	0.92
Al ₂ O ₃	1.86	18.02	2.39	16.81	6.39	17.01	9.51	12.80	3.90	16.46	4.07	13.07	14.84	6.64	1.12	16.22
FeO	0.65	0.86	1.46	0.92	1.06	0.86	1.92	1.17	1.18	0.83	1.18	0.92	0.92	1.87	0.57	0.84
Fe ₂ O ₃	0.57	0.86	1.48	13.63	2.30	10.69	4.58	7.08	1.47	9.54	1.54	10.31	10.40	1.81	0.54	8.28
MnO	0.11	0.09	0.07	0.11	0.19	0.15	0.16	0.18	0.11	0.16	0.14	0.18	0.13	0.12	0.07	0.15
MgO	0.88	2.12	0.99	2.03	2.52	2.38	2.12	2.85	1.74	3.24	2.09	2.87	2.93	2.23	0.35	2.71
CaO	0.26	2.15	0.26	2.21	0.60	2.65	1.48	1.69	0.43	2.12	0.59	1.94	1.67	0.82	0.19	2.46
Na ₂ O	0.30	3.28	0.54	3.78	1.49	3.64	2.57	2.80	0.94	2.13	0.90	3.26	1.95	1.21	0.15	1.86
K ₂ O	0.20	4.15	0.28	3.33	0.766	3.43	1.27	2.08	0.36	4.66	0.31	2.05	4.29	1.18	0.10	4.56
P ₂ O ₅	0.05	0.16	0.05	0.22	0.09	0.48	0.30	0.17	0.09	0.54	0.12	0.38	0.19	0.15	0.04	0.80
H ₂ O(-)	0.12	1.33	0.31	1.08	0.75	0.98	0.58	0.81	0.21	1.37	0.48	0.86	0.84	0.30	0.17	0.83
H ₂ O(+)	0.50	3.59	0.82	3.01	2.08	2.81	1.95	2.69	1.744	3.83	1.15	2.75	3.68	1.74	0.28	2.71
Res.	0.67	0.55	0.02	0.38	0.37	0.81	0.44	0.63	0.24	0.74	0.70	0.37	0.31	0.55	0.53	1.83
Co	15		11		29	20	23	34	20		26	35	24	28	5	
Ni	26		22		55	32	40	53	28		30	41	42	38	14	
Cu	23		15		100	180	120	160	52		75	160	22	530	11	
Zn	44		53		140	110	100	140	81		84	110	130	100	17	
Ga	5		4		12	23	15	18	7		6	17	24	12	3	
Rb	4		7		19	94	34	58	8		6	58	130	33	1	
Sr	28		38		94	280	170	210	53		51	240	160	100	18	
Y	9		7		16	40	26	25	10		15	53	33	20	5	
Zr	15		19		74	220	80	110	23		36	170	150	60	9	
Nb	4		5		6	10	7	9	5		5	12	11	5	3	
Pb	4		2		3	11	8	9	4		1	18	10	2	3	
Th	5		3		4	5	5	5	2		4	7	5	5	3	
Ba	37		58		150	390	190	240	110		85	310	340	190	88	
Name	32	33	34	35	36	37	38	39	40	40a	40b	40c	41	42	43	
	Chert	Shale	Chert	Shale	Chert	Shale	Chert	Shale	Chert	Shale	Chert	Shale	Chert	Shale	Chert	
SiO ₂	89.36	66.68	87.26	53.53	88.09	53.34	85.63	67.45	89.96	53.66	77.31	54.72	88.08	61.60	95.47	
TiO ₂	0.18	1.06	0.23	1.86	0.20	1.52	0.25	1.05	0.19	2.32	0.48	1.34	0.22	1.37	0.04	
Al ₂ O ₃	4.01	11.10	4.54	18.08	4.21	17.23	5.17	11.97	3.47	15.28	7.99	16.47	3.93	13.29	1.41	
FeO	0.93	1.48	1.44	0.98	1.47	1.50	1.87	1.98	1.33	1.75	2.62	2.68	1.32	1.92	0.43	
Fe ₂ O ₃	1.29	8.10	1.58	10.18	1.12	8.78	1.30	6.08	1.05	10.10	3.07	7.04	1.59	7.32	0.37	
MnO	0.11	0.16	0.11	0.15	0.12	0.12	0.12	0.15	0.07	0.13	0.17	0.17	0.09	0.12	0.02	
MgO	1.34	2.65	2.03	2.21	2.26	2.53	2.35	2.68	1.26	2.76	3.16	3.17	1.54	1.94	0.26	
CaO	0.75	2.09	0.58	3.48	0.46	3.02	0.73	2.05	0.45	3.25	1.09	2.74	0.39	1.79	0.21	
Na ₂ O	0.75	2.47	0.89	4.64	0.95	4.11	1.25	3.00	0.82	3.28	1.85	4.67	1.02	5.38	0.00	
K ₂ O	0.39	1.83	0.50	2.77	0.26	2.79	0.36	1.48	0.24	2.65	0.75	1.83	0.35	1.00	0.24	
P ₂ O ₅	0.15	0.50	0.14	0.46	0.11	0.32	0.15	0.27	0.10	0.38	0.19	0.27	0.14	0.44	0.02	
H ₂ O(-)	0.18	0.40	0.05	0.53	0.03	0.71	0.18	0.43	0.09	0.83	0.31	0.69	0.33	0.64	0.21	
H ₂ O(+)	1.12	1.23	1.16	3.04	1.36	1.94	1.30	2.44	1.00	2.76	2.30	2.96	1.25	1.58	0.54	
Res.	0.73	2.00	0.88	1.03	0.80	1.61	0.65	0.81	0.28	0.74	0.67	0.63	0.36	0.85	0.13	
Co	12		12	18	17	16	21	9	7	12	18	20	7	8	4	
Ni	22		24	24	23	23	27	23	15	20	30	41	19	24	12	
Cu	93		86	280	65	2240	99	150	28	150	92	200	30	110	8	
Zn	46		60	82	65	91	72	82	36	80	98	130	46	65	16	
Ga	7		9	21	8	21	9	17	6	21	14	19	7	13	3	
Rb	8		13	72	4	73	9	39	4	70	17	44	8	26	4	
Sr	71		71	330	54	340	81	230	60	260	130	360	46	250	16	
Y	13		15	65	12	43	13	39	10	67	21	38	13	47	4	
Zr	28		38	220	31	190	38	150	26	290	63	160	32	150	9	
Nb	4		6	10	5	7	6	9	4	15	6	9	5	10	2	
Pb	3		3	11	8	10	9	5	8	11	3	10	3	8	1	
Th	4		3	7	1	5	4	5	2	7	5	6	5	6	2	
Ba	140		180	590	91	300	110	270	74	430	240	410	65	230	13	

Table 2. Averaged chemical compositions of cherts and associated shales, on water and others free basis, from the Shimanto, Mino (Yamamoto, 1983), and Franciscan (Yamamoto, 1987) terranes with their standard deviations. Oxides are expressed in % and metals are in ppm.

Lithology No	SHIMANTO		MINO		FRANCISCAN	
	Chert 22	Shale 24	Chert 71	Shale 42	Chert 88	Shale 28
SiO ₂	87.79 ± 5.93	58.95 ± 4.84	95.19 ± 3.46	63.96 ± 7.22	92.63 ± 2.92	58.95 ± 9.85
TiO ₂	0.25 ± 0.15	1.47 ± 0.40	0.10 ± 0.10	0.75 ± 0.21	0.09 ± 0.05	1.21 ± 0.90
Al ₂ O ₃	4.71 ± 2.41	15.95 ± 2.20	1.97 ± 1.35	15.97 ± 3.72	1.41 ± 1.02	12.15 ± 3.63
FeO	1.29 ± 0.52	1.24 ± 0.54	0.50 ± 0.19	2.35 ± 1.37	0.26 ± 0.13	1.26 ± 1.68
Fe ₂ O ₃	1.79 ± 1.08	9.59 ± 1.94	0.63 ± 0.38	3.62 ± 1.42	2.67 ± 1.71	14.69 ± 7.00
MnO	0.11 ± 0.04	0.16 ± 0.03	0.03 ± 0.03	0.28 ± 0.70	0.80 ± 1.17	3.96 ± 7.57
MgO	1.62 ± 0.75	2.68 ± 0.47	0.53 ± 0.39	2.47 ± 0.68	0.33 ± 0.27	3.03 ± 1.26
CaO	0.67 ± 0.45	2.71 ± 0.82	0.38 ± 0.08	0.26 ± 0.41	0.11 ± 0.06	1.59 ± 3.14
Na ₂ O	1.03 ± 0.64	3.58 ± 1.22	0.09 ± 0.06	0.31 ± 0.41	0.16 ± 0.19	0.59 ± 0.99
K ₂ O	0.57 ± 0.39	3.03 ± 1.21	0.51 ± 0.42	4.68 ± 1.11	0.42 ± 0.33	3.87 ± 2.05
P ₂ O ₅	0.14 ± 0.08	0.56 ± 0.44	0.06 ± 0.08	0.27 ± 0.28	0.03 ± 0.02	0.14 ± 0.10
Co	16 ± 7.4	22 ± 9.3	3.3 ± 2.2	17 ± 11	3.5 ± 2.4	18 ± 12
Ni	29 ± 11	39 ± 16	14 ± 5.4	66 ± 22	16 ± 16	70 ± 48
Zn	68 ± 32	110 ± 28	30 ± 15	160 ± 56	43 ± 82	160 ± 70
Ga	8.3 ± 3.5	21 ± 3.6	3.3 ± 2.5	25 ± 6.2	1.7 ± 1.8	19 ± 6.1
Rb	14 ± 11	77 ± 34	29 ± 24	210 ± 45	9.0 ± 9.0	110 ± 62
Sr	70 ± 39	260 ± 67	39 ± 54	53 ± 36	25 ± 1.2	41 ± 23
Y	15 ± 7.4	47 ± 12	6.7 ± 8.4	38 ± 23	9.0 ± 5.5	63 ± 20
Zr	41 ± 24	180 ± 39	23 ± 23	164 ± 47	27 ± 12	180 ± 44
Nb	5.4 ± 1.5	11 ± 2.5	2.7 ± 1.9	14 ± 3.4	3.3 ± 1.5	13 ± 4.4
Pb	3.9 ± 2.6	11 ± 3.8	8.2 ± 6.0	29 ± 34	25 ± 15	78 ± 85
Th	4.0 ± 1.4	6.4 ± 1.4	3.3 ± 3.1	18 ± 7.4	3.3 ± 2.9	14 ± 7.9

those in the Mino bedded cherts. Since basalts are plotted in a field near that of shales, lithogenic materials in shales may have originated partly from the basal basalt. Petrologic observations confirm this interpretation; the Shimanto shales contain microcrystalline sphene and large amounts of basaltic fragments with much TiO₂. The contribution of basaltic fragments, containing relatively large amounts of plagioclase, to the Shimanto shales also causes the enrichments of CaO (2.71%), Na₂O (3.58%) and Sr (260 ppm) compared with the Mino (0.26%, 0.31% and 53 ppm, respectively) and Franciscan shales (1.59%, 0.59% and 41 ppm, respectively).

The Franciscan cherts and shales are extremely enriched in total Fe₂O₃ and MnO in comparison with the Shimanto and Mino cherts and shales (Table 2

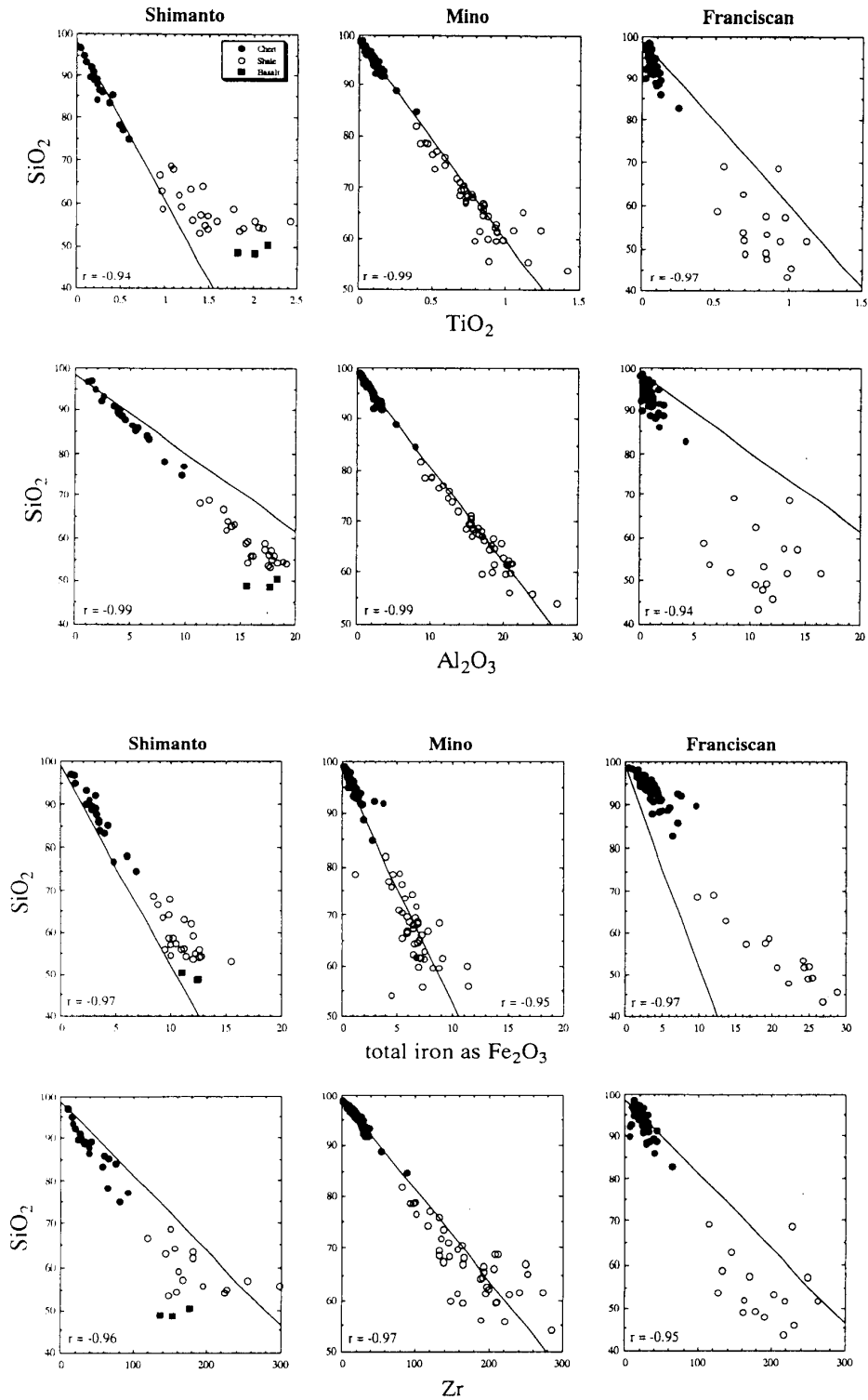


Fig. 2. Plots of SiO₂ versus TiO₂, Al₂O₃, total iron as Fe₂O₃ and Zr for cherts (closed circle) and shale partings (open circle) from the Shimanto, Mino (Yamamoto, 1983) and Franciscan (Yamamoto, 1987) terranes. Solid squares show basal pillow basalt. Regression lines in all diagrams are calculated by the method of least squares for the Mino cherts and shales. Correlation coefficients calculated for cherts and shales are shown in the lower left of each diagram.

and Fig. 2). As Yamamoto (1987) and Murray et al. (1990, 1991) pointed out, the Franciscan bedded cherts, particularly lower-horizon bedded cherts, are subjected to intense hydrothermal activities. It is well known that hydrothermal deposits are enriched in total Fe_2O_3 , MnO , and some transition elements (e.g. Piper, 1973; Bonatti et al., 1979; Adachi et al., 1986; Sugitani et al., 1991). The enrichment of these hydrothermal elements lowers concentrations of lithogenic elements such as TiO_2 , Al_2O_3 , Zr, etc. The Franciscan bedded cherts are thus plotted in the field below the regression lines for the Mino bedded cherts (Fig. 2).

Compositional variation against depositional horizon

During the diagenetic process, chemical fractionation between cherts and shales may have occurred. According to Murray (1994), at least Ca, Mg, Sr, P, Ba, and Mn are remobilized and removed from proto-chert to host sediment during silicification of carbonate sediments. Hein and Karl (1983) emphasized that cherts formed by replacement of calcareous sediments, usually occurring as nodules or lenses, are not analogous to the orogenic cherts like the Shimanto bedded cherts. Since the precursor materials of the Shimanto bedded cherts comprising numerous radiolarian tests are not carbonate but are instead silicate, chemical fractionations different from those reported by Murray (1994) may have operated in the Shimanto bedded cherts.

To discuss the chemical fractionation between cherts and shales, some representative elements of the Shimanto cherts and shales are plotted against vertical distance from the basal pillow-basalt (Fig. 3). Among the lithogenic major elements, only Al, Ti and Fe are believed to be little affected during diagenetic and weathering processes (e.g. Sugisaki et al., 1978; Yamamoto et al., 1986; Murray, 1994). If the rhythmic chert-shale repetition of bedded cherts is formed by the diagenetic migration of SiO_2 from proto-shale to proto-chert (Murray et al., 1992), elemental ratio of immobile Al and Ti in cherts and shales remains constant throughout the horizon. In Shimanto samples, the average ratios of the $\text{Al}_2\text{O}_3/\text{TiO}_2$ ratio are 21.1 and 11.4 for cherts and shales, respectively. This may be ascribed to compositional difference of lithogenic materials contained in cherts from those in shales because of the immobility of Al and Ti. As stated in the former section, the predominant contribution of basaltic fragments and Ti-bearing minerals to the Shimanto shales enhances the TiO_2 content in comparison with the Mino shales. The basal pillow-basalt shows low $\text{Al}_2\text{O}_3/\text{TiO}_2$ ratio from 8.45 to 8.79. The low $\text{Al}_2\text{O}_3/\text{TiO}_2$ ratio of shales, therefore, comes from the basaltic components and Ti-bearing mineral, sphene. In other words, the cherts with high $\text{Al}_2\text{O}_3/\text{TiO}_2$ ratio, except for some cherts with low one, are considered to be less contributed by the basal basalts.

Like the case of $\text{Al}_2\text{O}_3/\text{TiO}_2$, the Shimanto cherts show high $\text{MnO}/\text{Al}_2\text{O}_3$ ratio of 0.022 on average, whereas in shales the ratio is as low as 0.010 (Fig. 3). The $\text{MnO}/\text{Al}_2\text{O}_3$ ratio in basal pillow-basalts ranges from 0.010 to 0.012,

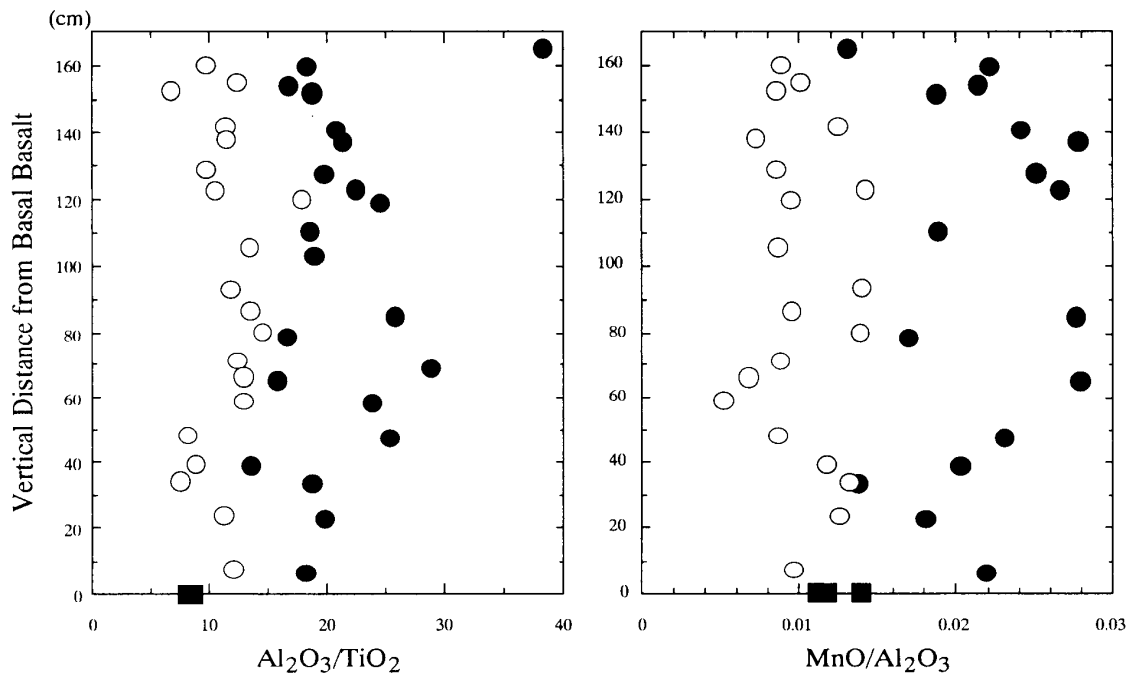


Fig. 3. Vertical variations of $\text{Al}_2\text{O}_3/\text{TiO}_2$ and $\text{MnO}/\text{Al}_2\text{O}_3$ ratios for cherts (closed circles), shales (open circles) and basal basalt (solid squares) from the Shimanto terrane.

which is close to that of shales. It is therefore interpreted that the contributions of basaltic components decrease the $\text{MnO}/\text{Al}_2\text{O}_3$ ratio of shales.

Thus, in the Shimanto rocks, the difference of clastic materials in cherts and shales obscures the chemical fractionation during diagenetic processes.

Hydrothermal contribution to the Shimanto “accreted bedded cherts”

Geochemical characteristics of hydrothermal deposits around active ocean ridges have been reported by many researchers (e.g. Boström and Peterson, 1969; Bonatti et al., 1972; Mills et al., 1993; German et al., 1993). These authors have emphasized that sediments deposited around an active ocean ridge contain large amounts of hydrothermal emanations; for example, surface sediments collected at a point 1250 km west of the East Pacific Rise during DSDP Leg 92 contain about 75% hydrothermal precipitate and 25% detrital silicate on a water- and carbonate-free basis (Marchig and Erzinger, 1986). If the Shimanto pillow basalt had originated from subducting oceanic-ridge basalt (Taira et al., 1980, 1985), the overlying bedded cherts should have been subjected to intense hydrothermal activities similar to those shown by the Franciscan bedded cherts (Yamamoto, 1987; Murray et al., 1990, 1991).

The hydrothermal contribution to the Shimanto bedded cherts were scrutinized on the Al-Fe-Mn diagram by comparison with various deposits, such as non-hydrothermal biogenic Mino bedded cherts, hydrothermal Franciscan bedded cherts, metalliferous deposits around active ocean ridges and argillaceous marine sediments (Fig. 4). On the diagram, the Mino bedded cherts as

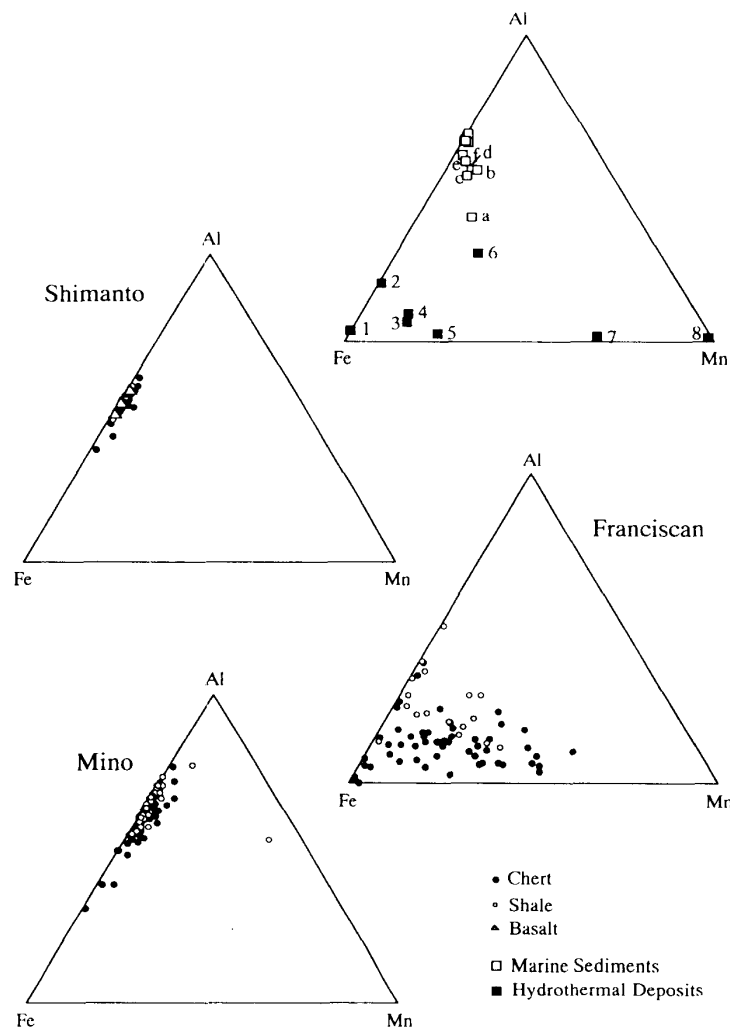


Fig. 4.

Al-Fe-Mn diagram showing the contribution of hydrothermal emanations. Sample symbols: closed circles = cherts; open circles = shales; open triangles = basal pillow basalts; closed squares = hydrothermal deposits around active ocean ridges – 1. TAG Hydrothermal mound, 26°08'N, Mid-Atlantic Ridge, average of samples (German et al., 1993), 2. Galapagos Hydrothermal Mounds Field during DSDP Leg 70, five samples (Moorby, 1983), 3. sediments west of East Pacific Rise, upper part of DSDP Leg 92, 52 samples (Marchig and Erzinger, 1986), 4. Metal-rich sediment in the West Philippine Basin during DSDP Leg 31, 22 samples (Bonatti et al., 1979), 5. sediments west of East Pacific Rise, lower part of DSDP Leg 92, 64 samples (Marchig and Erzinger, 1986), 6. East Pacific Rise sediments at about 12–14°S between 90° and 140°W, average of 19 samples (Boström and Peterson, 1969), 7. hydrothermal mounds near the Galapagos Rift, 26 samples (Corliss et al., 1978) and 8. Mn beds from the northern Afar Rift, Ethiopia, six samples (Bonatti et al., 1972); open squares = argillaceous marine sediments – a. the central Pacific, southern part of GH80-1, samples (Sugisaki and Kinoshita, 1982), b. sediments from central Pacific around 10°N and 170°W, GH80-5, 109 samples (Sugisaki and Yamamoto, 1984), c. the central Pacific, northern part of GH80-1, samples (Sugisaki and Kinoshita, 1982), d. central Pacific sediment around 3°N and 169°W, GH81-4, 55 samples (Yamamoto and Sugisaki, 1986), e. and f. around the Izu-Ogasawara Trench, GH79-2, 3 and 4, 21 and 46 samples, respectively (Sugisaki and Kinoshita, 1981). Others are sediments around the Japanese Islands; GH75-4, 28 samples (Sugisaki, 1978), GH78-2, 67 samples (Sugisaki, 1979), DSDP Leg 56/57 Sites 438 and 439, 48 and 11 samples, respectively, (Sugisaki, 1980a), DSDP Leg 58 Site 442A, 78 samples (Sugisaki, 1980b) and GH77-3, 81 samples, (Sugisaki, 1996).

well as most argillaceous marine sediments from various environments plot into an area of low Mn content. Because of lack of sign for hydrothermal activity on these samples, the plotted area is regarded as non-hydrothermal. On the other hand, hydrothermal deposits around active ocean ridges and hydrothermal Franciscan bedded cherts are characterized by enrichments of Fe, Mn, and some transition elements, and they plot outside the non-hydrothermal area on the diagram. The Shimanto cherts and shales are not conspicuously enriched in Fe and Mn (Table 2) and plotted in the Mn-poor area along the Al-Fe axis on the Al-Fe-Mn diagram. The Shimanto bedded cherts are slightly enriched in Fe compared with the Mino bedded cherts and argillaceous marine sediments. This Fe enrichment is attributed to the contribution of basaltic fragments, as pointed out previously, and this feature is indicated by basal pillow-basalt plotted in the area of the Shimanto bedded cherts on the diagram. The examination on Al-Fe-Mn diagram shows that the Shimanto bedded cherts had deposited in the marine environment free from hydrothermal activities.

Another approach to the problem was made on other discriminate diagrams that are suggested by Murray (1994) who compiled geochemical data presented in the literature for chert sequences from 49 localities around the world (Fig. 5). On these diagrams, Al_2O_3 and TiO_2 are indicators of

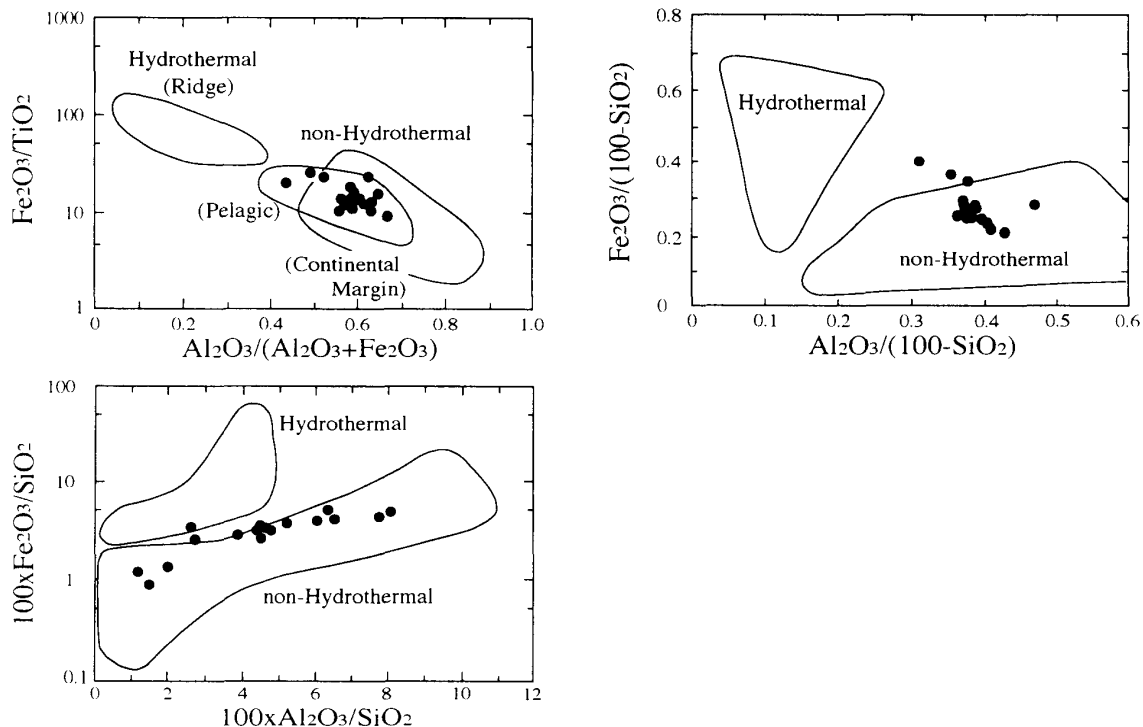


Fig. 5. Discriminant diagrams, $\text{Fe}_2\text{O}_3/$ versus $\text{Al}_2\text{O}_3/(\text{Al}_2\text{O}_3 + \text{Fe}_2\text{O}_3)$, $\text{Fe}_2\text{O}_3/(100 - \text{SiO}_2)$ versus $\text{Al}_2\text{O}_3/(100 - \text{SiO}_2)$ and $100 \times \text{Fe}_2\text{O}_3/\text{SiO}_2$ versus $100 \times \text{Al}_2\text{O}_3/\text{SiO}_2$ proposed by Murray (1994). Almost all the Shimanto cherts are plotted into the region of continental margin or pelagic.

terrigenous input because of their affiliation with aluminosilicate phases; Fe_2O_3 (total iron as Fe_2O_3) is an indicator of hydrothermal input at oceanic spreading centers, as mentioned before. On the three diagrams, the Shimanto cherts are not plotted in the area indicating ocean-ridge regions. This reinforces the above inference based on the Al-Fe-Mn diagram.

Depositional environments of the Shimanto “accreted bedded cherts”

Depositional environments of the bedded cherts cannot be exactly estimated by Murray’s diagrams, because pelagic cherts are similar to continental margin cherts with respect to relative abundances among Ti, Al, Fe and Si. On the contrary, Sugisaki et al. (1982), Yamamoto (1983) and Sugisaki (1984) emphasized that hydrogenous elements such as Mn and Co is useful in evaluation of sedimentary environments. Murray (1994), however, suggested that MnO is not a reliable tracer of hydrogenous input, because Mn is remobilized from proto-chert to host sediment during chert formation. If this holds true for bedded cherts, $\text{MnO}/\text{Al}_2\text{O}_3$ or MnO/TiO_2 ratio of cherts must be less than that of host sediments, namely shale partings. Nevertheless the Figure 2 depicted by Murray et al. (1992) indicates that the Mn/Al ratio as same as Ti/Al ratio in cherts normalized to that in shale partings of bedded cherts from 6 various locations is around 1. According to Sugisaki et al. (1982), Mino cherts show higher MnO/TiO_2 ratio (0.25, average of 69 samples) than do shale partings (0.17, that of 37 samples). These facts suggest that clear fractionation of Mn between cherts and host sediments cannot be recognized for bedded cherts.

On the contrary, Mn mobilization during early stage of diagenetic processes are widely discussed (e.g. Goldberg and Arrhenius, 1958; Lynn and Bonatti, 1965; Sugisaki, 1984). In this context, we re-examine the mobility of Mn on the basis of data of cored marine sediments at the Pacific margin of Southwest Japan, GH75-4 (Sugisaki, 1978), the Yamato Bank in the Sea of Japan, GH78-2 (Sugisaki, 1979) and the Central Pacific Basin, GH81-4 (Yamamoto and Sugisaki, 1986).

Hitherto we have used TiO_2 -normalized values for the discussion of genetic relation of siliceous rocks with their associated rocks (Sugisaki et al., 1982; Sugisaki, 1984). The Shimanto shales, however, contain abundant sphene and accordingly their TiO_2 content is anomalously high compared with the Mino and Franciscan shales. Thus we selected Al_2O_3 for normalization because it is immobile during usual sedimentary processes. The Mn distribution in marine sediments is controlled predominantly by redox condition of the environment and sedimentation rate (e.g. Goldberg and Arrhenius, 1958; Sugisaki, 1984). The more oxidized are marine environments, the more abundant becomes MnO content in the sediments. Because both quantities of land-derived clastic substances and organic matters as a reducing reagent decrease with increase of distance from land, pelagic sediments show high $\text{MnO}/\text{Al}_2\text{O}_3$ ratio whereas nearshore sediments do low ratio. As shown in the Fig. 6, GH75-4 samples deposited in hemipelagic environments show relatively low and uniform

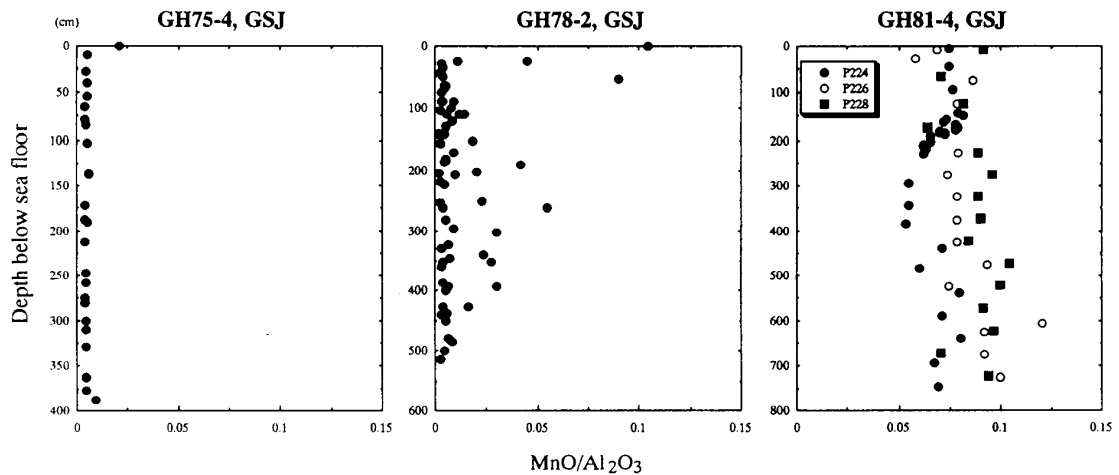


Fig. 6. Vertical variation of $\text{MnO}/\text{Al}_2\text{O}_3$ ratio against depth below sea floor for sediments during GH75-4 (Sugisaki, 1978), GH78-2 (Sugisaki, 1979) and GH81-4 (Yamamoto and Sugisaki, 1986), Geological Survey of Japan.

$\text{MnO}/\text{Al}_2\text{O}_3$ ratios around 0.005. On the contrary, GH81-4 samples deposited in pelagic environments have high ratio of $\text{MnO}/\text{Al}_2\text{O}_3$ around 0.08 with the large fluctuation. The chemical signature of depositional environment, therefore, is well preserved throughout core depth (Fig. 6). In the core section of GH78-2 samples, spikes of $\text{MnO}/\text{Al}_2\text{O}_3$ ratio as high as 0.1 appear in some horizons. Since granite and basalt show the $\text{MnO}/\text{Al}_2\text{O}_3$ ratio about 0.012 and 0.003 (Taylor, 1964), respectively, only the variation of mixing ratio of granitic and basaltic clastics cannot cause the spikes.

Many reports indicate that pore fluids containing Mn^{2+} at depth of reducing conditions is expelled upward during sedimentation compaction and that the fluid precipitates MnO_2 near sediment surface under oxic conditions (e.g. Lynn and Bonatti, 1965). This process is possibly responsible for the high $\text{MnO}/\text{Al}_2\text{O}_3$ ratio of the uppermost samples in the GH75-4 and GH78-2. In contrast the spike-like enrichments of Mn at several horizons in GH98-2 core, excepting the surface sediments, may be resulted from formation of manganese carbonate bands. Sugisaki et al. (1991) emphasized that the manganese carbonate band is characteristic of hemipelagic marine sediments and is a good indicator of hemipelagic sedimentary environments. Excepting anomalously high $\text{MnO}/\text{Al}_2\text{O}_3$ ratio at some horizons containing manganese carbonate, GH78-2 samples show rather small ratio in comparison with pelagic GH81-4 samples. As shown in Fig. 7, the $\text{MnO}/\text{Al}_2\text{O}_3$ ratio of marine argillaceous sediments continuously increases as the distance from land increases. This fact shows that the $\text{MnO}/\text{Al}_2\text{O}_3$ ratio can be a good indicator of sedimentary environments, although the mobility of Mn in a specific environment such as the reductive conditions should be taken into account.

Because the $\text{MnO}/\text{Al}_2\text{O}_3$ ratio of the Shimanto shales is lowered by the contribution of the basal basalt, as described above, the ratio of the shales may not reflect their depositional environment. In contrast, the Shimanto cherts

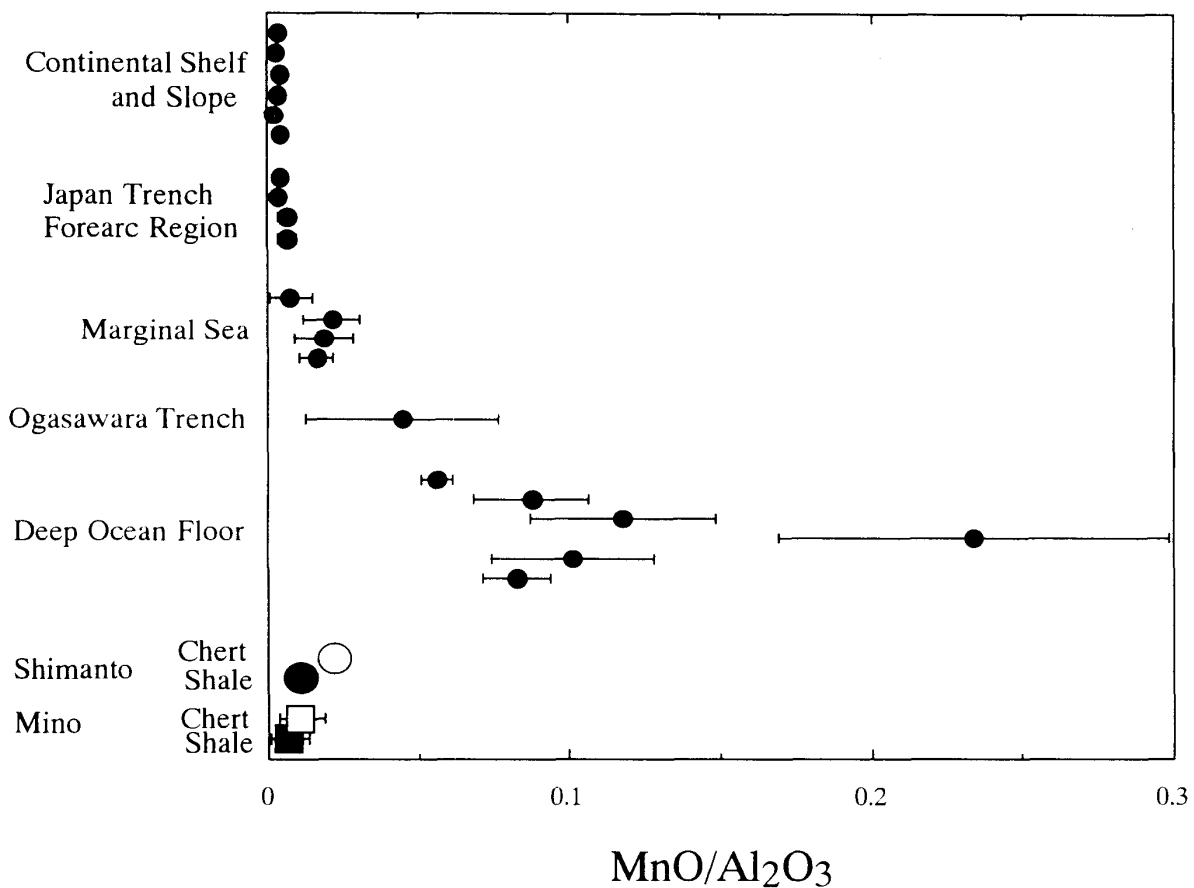


Fig. 7. Comparison of MnO/Al_2O_3 ratio of Cretaceous Shimanto cherts with those of marine argillaceous sediments in various environments. The horizontal line indicates ± 1 sigma. Data sources are the same as Figure 4.

are less affected by the basal basalt (Fig. 2). If we compare the averaged value of MnO/Al_2O_3 of the Shimanto cherts to those of marine argillaceous sediments (Fig. 7), it is deduced that the Shimanto bedded cherts are more akin to the marginal-sea sediments but not to pelagic sediments.

CONCLUDING REMARKS

As to the origins and depositional environments of the Shimanto bedded cherts, Taira et al. (1980) emphasized that the allochthonous bodies including bedded cherts and pillow-basalts in the terrane have deposited in the low-latitude ocean-ridge region and accreted to the Japanese Island Arc; the basis of their conclusion is 1) paleomagnetic data of basaltic rocks and sediments indicating shallow inclinations, 2) occurrence of bedded cherts generally considered to be pelagic and other geologic data. Their conclusion clearly conflicts with ours, and the cause of the inconsistency should be demonstrated.

If the allochthonous bodies are accreted at a subduction zone where orogenic activity is high, they may suffer thermal and/or chemical alteration that could alter their magnetic properties. Larson et al. (1982) showed that a

stable chemical remanent magnetization are acquired during diagenetic processes over a geologic period. It is well accepted that rocks of several million years old contain more than one magnetic component. Hagstrum and Murchey (1996) pointed out the possibility that overprinted component (component B in their definition) was incorrectly interpreted as the primary magnetization. In order to unravel a component that carries primary magnetization and to delineate the magnetic properties of the Shimanto rocks, more detailed paleomagnetic studies must be needed, as pointed out by Shibuya and Sasajima (1986).

Although many bedded cherts are believed to be deposited in low-latitude high-productivity region, bedded cherts with various depositional environments are reported; continental margin, deep ocean floor, and spreading ridge proximal (e.g. Sugisaki et al., 1982; Yamamoto, 1987; Aitchison and Flood, 1990; Murray et al., 1990). Jenkyns and Winterer (1982) emphasized that pelagic nodular and lenticular cherts are not identical with Cenozoic bedded (ribbon) cherts on land in occurrence. Yamamoto (1987) reported that bedded cherts from the Shimanto terrane in the Kii Peninsula, Southwest Japan, contain a considerable amount of hydrothermal components compared with the bedded cherts studied here. However, the bedded cherts are accompanied by thick acidic tuffs, regarded generally as a product of rhyolitic and dacitic volcanisms in mobile belts, and hence they may have accumulated in a hemipelagic environment such as a marginal basin or an inter-arc basin (Yamamoto, 1987). Consequently, the Shimanto rocks are inferred to have deposited in a hemipelagic environment. This shows that the siliceous deposits associated with pillow basalt in orogenic belts are not necessarily akin to sediments around spreading oceanic ridges.

ACKNOWLEDGMENTS

We wish to express our gratitude to Mr. S. Yogo, Nagoya University, who made thin sections and to Dr. H. Maekawa, Kobe University, who operated scanning electron microprobe. We also thank Dr. Y. Otofuji, Kobe University, for valuable information and comments on the paleomagnetic studies. We are further indebted to Dr. R. Sugisaki, Meijo University, for critical reading of manuscript.

REFERENCES

- Adachi, M., Yamamoto, K. and Sugisaki, R., 1986. Hydrothermal chert and associated siliceous rocks from the northern Pacific: their significance as indication of ocean ridge activity. *Sediment. Geol.*, **47**, 125–148.
- Aitchison, J.C. and Flood, P.G., 1990. Geochemical constraints on the depositional setting of Palaeozoic cherts from the New England orogen, NSW, eastern Australia. *Marine Geol.*, **94**, 79–95.
- Bonatti, E., Fisher, D.E., Joensuu, O., Rydell, H. and Beyth, M., 1972. Iron-Manganese-Barium deposit from the northern Afar Rift (Ethiopia). *Econ. Geol.*, **67**, 717–730.

- Bonatti, E., Kolla, V., Moore, W.S. and Stern, C., 1979: Metallogenesis in marginal basins: Fe-rich basal deposits from the Philippine Sea. *Earth Planet. Sci. Lett.*, **32**, 21–37.
- Boström, K. and Peterson, M.N.A., 1969: The origin of aluminum-poor ferromanganous sediments in areas of high heat flow on the East Pacific Rise. *Marine Geol.*, **7**, 427–447.
- Corliss, J.B., Lyle, M., Dymond, J. and Crane, K., 1978. The geochemistry of hydrothermal mounds near the Galapagos Rift. *Earth Planet. Sci. Lett.*, **40**, 12–24.
- German, C.R., Higgs, N.C., Thomson, J., Mills, R., Elderfield, H., Blusztajn, J., Fleer, A.P. and Bacon, M.P., 1993. A geochemical study of metalliferous sediment from the TAG Hydrothermal Mound, 26-08'N, Mid-Atlantic Ridge. *Jour. Geophys. Res.*, **98**, 9683–9692.
- Goldberg, E.D. and Arrhenius, G.O.S., 1958. Chemistry of Pacific pelagic sediments. *Geochim. Cosmochim. Acta*, **13**, 153–212.
- Hagstrum, J.T. and Murchey, B.L., 1996. Paleomagnetism of Jurassic radiolarian chert above the Coast Range ophiolite at Stanley Mountain, California, and implications for its paleogeographic origins. *Geol. Soc. Am. Bull.*, **108**, 643–652.
- Hayashida, A., Otofujii, Y. and Torii, M., 1988. Palaeoposition of Southwest Japan and convergence between Eurasia and Pacific plates in pre-Neogene time. *Modern Geol.*, **12**, 467–480.
- Hein, J.R. and Karl, S.M., 1983. Comparisons between open-ocean and continental margin chert sequences. In: A. Iijima, J.R. Hein and R. Siever (Eds.), *Siliceous Deposits in the Pacific Region*. (Development of Sedimentology, 36), Elsevier, Amsterdam, pp.25–43.
- Hirooka, K., Nakajima, T., Sakai, H., Date, T., Nittamachi, K. and Hattori, I., 1983. Accretion tectonics inferred from paleomagnetic measurements of Paleozoic and Mesozoic rocks in central Japan. In: M. Hashimoto and S. Uyeda (Editors), *Tectonics in the Circum-Pacific Regions*. TERRAPUB, Tokyo, pp.179–194.
- Kodama, K., Taira, A., Okumura, M. and Saito, Y., 1983. Paleomagnetism of the Shimanto Belt in Shikoku, Southwest Japan. In: M. Hashimoto and S. Uyeda (Editors), *Tectonics in the Circum-Pacific Regions*. TERRAPUB, Tokyo, pp.231–241.
- Jenkyns, H.C. and Winterer, E.L., 1982. Palaeoceanography of Mesozoic ribbob radiolarites. *Earth Planet. Sci. Lett.*, **60**, 351–375.
- Larson, E.E., Walker, T.R., Patterson, P.E. Hoblitt, R.P. and Rosenbaum, J.G., 1982. Paleomagnetism of the Moenkopi formation, Colorado plateau: Basis for long-term model of acquisition of chemical remanent magnetism in red beds. *Jour. Geophys. Res.*, **87**, 1082–1106.
- Lynn, D.C. and Bonatti, E., 1965. Mobility of manganese in diagenesis of deep-sea sediments. *Marine Geol.*, **3**, 457–474.
- Marchig, V. and Erzinger, J., 1986. Chemical composition of Pacific sediments near 20°N: Changes with increasing distance from the East Pacific Rise. In: M. Leinen, D.K. Rea et al. (Editors), *Init. Repts. DSDP*, 92: U.S. Govt. Printing Office, Washington, 371–381.
- Mills, R., Elderfield, H. and Thomson, J., 1993. A dual origin for the hydrothermal component in a metalliferous sediment core from the Mid-Atlantic Ridge. *Jour. Geophys. Res.*, **98**, 9671–9681.
- Moorby, S.A., 1983. The geochemistry of transitional sediments recovered from the Galapagos Hydrothermal Mounds Field during DSDP Leg 70-implications for mounds formation. *Earth Planet. Sci. Lett.*, **62**, 367–376.
- Murray, R.W., 1994. Chemical criteria to identify the depositional environment of chert: general principles and applications. *Sediment. Geol.*, **90**, 213–232.
- Murray, R.W., Buchholtz ten Brink, M.R., Jones, D.L. Gerlach, D.C. and Russ, G.P., III, 1990. Rare earth elements as indicators of different marine depositional environments in chert and shale. *Geology*, **18**, 268–271.

- Murray, R.W., Buchholtz ten Brink, M.R., Gerlach, D.C., Russ, G.P., III and Jones, D.L. 1991. Rare earth, major and trace elements in chert from the Franciscan Complex and Monterey Group, California: assessing REE sources to fine-grained marine sediments. *Geochim. Cosmochim. Acta*, **55**, 1875–1895.
- Murray, R.W., Jones, D.L. and Buchholtz ten Brink, M.R., 1992. Diagenetic formation of bedded chert: Evidence from chemistry of the chert-shale couplet. *Geology*, **20**, 271–274.
- Piper, D.Z., 1973. Origin of metalliferous sediments from the East Pacific Rise. *Earth Planet. Sci. Lett.*, **19**, 75–82.
- Shibuya, H. and Sasajima, S., 1986. Paleomagnetism of red chert: a case study in the Inuyama area, central Japan. *J. Geophys. Res.*, **91**, 14105–14116.
- Shimizu, H. and Masuda, A., 1977. Cerium in chert as an indication of marine environment of its formation. *Nature*, **266**, 346–348.
- Shimizu, H., Amano, M. and Masuda, A., 1991, La-Ce and Sm-Nd systematics of siliceous sediment: A clue to marine environment in their deposition. *Geology*, **19**, 369–371.
- Sugisaki, R., 1978. Chemical composition of argillaceous sediments on the Pacific Margin of southwest Japan. *Geol. Surv. Japan Cruise Rept.*, **9**, 65–73.
- Sugisaki, R., 1979. Chemical composition of argillaceous sediments around the Yamato Bank in the Japan Sea. *Geol. Surv. Japan Cruise Rept.*, **13**, 65–88.
- Sugisaki, R., 1980a. Major element chemistry of the Japan Trench sediments, Legs 56 and 57, Deep Sea Drilling Project. In: M. Lee and L.N. Stout (Editors), *Init. Repts. DSDP*, 56/57: U.S. Govt. Printing Office, Washington, 1233–1249.
- Sugisaki, R., 1980b. Major-element chemistry of argillaceous sediments at Deep Sea Drilling Project Sites 442, 443 and 444, Shikoku Basin. In: G. de Vries Klein, K. Kobayashi et al. (Editors), *Init. Repts. DSDP*, 58: U.S. Govt. Printing Office, Washington, 719–735.
- Sugisaki, R., 1984. Relationship between chemical composition and sedimentation rate of Pacific ocean-floor sediments deposited since the middle Cretaceous: Basic evidence for chemical constraints on depositional environments of ancient sediments. *J. Geol.*, **92**, 235–259.
- Sugisaki, R., 1996. Chemical composition of argillaceous sediments around the Nishitsugaru Basin in the Japan Sea. *Geol. Surv. Japan Cruise Rep.* (in press)
- Sugisaki, R. and Kinoshita, T., 1981. Chemical composition of marine argillaceous sediments around the Izu-Ogasawara Islands. *Geol. Surv. Japan Cruise Rep.*, **14**, 146–158.
- Sugisaki, R. and Kinoshita, T., 1982. Major element chemistry of the sediments on the central Pacific transect, Wake to Tahiti, GH80-1 Cruise. *Geol. Surv. Japan Cruise Rep.*, **18**, 294–313.
- Sugisaki, R. and Yamamoto, K., 1984. Major element chemistry of Pacific marine sediments around 10-N and 174-W samples for GH80-5 Cruise. *Geol. Surv. Japan Cruise Rep.*, **21**, 195–208.
- Sugisaki, R., Yamamoto, K. and Adachi, M., 1982. Triassic bedded cherts in central Japan are not pelagic. *Nature*, **298**, 644–647.
- Sugisaki, R., Ohashi, M., Sugitani, K. and Sugisaki, R., 1987. Compositional variations in manganese micronodules: A possible indicator of sedimentary environments. *J. Geol.*, **95**, 433–454.
- Sugisaki, R., Sugitani, K. and Adachi, M., 1991. Manganese carbonate bands as an indicator of hemipelagic sedimentary environments. *J. Geol.*, **99**, 23–40.
- Sugitani, K., Sano, H., Adachi, M. and Sugisaki, R., 1991: Permian hydrothermal deposits in the Mino Terrane, central Japan: implications for hydrothermal plumes in an ancient basin. *Sediment. Geol.*, **71**, 59–71.

- Taira, A., Okamura, M., Katto, J., Tashiro, M., Saito, Y., Hashimoto, M., Chiba, T. and Aoki, T., 1980. Lithofacies and geologic age relationship within melange zones of Northern Shimanto Belt (Cretaceous), Kochi Prefecture, Japan. In: A. Taira and M. Tashiro (eds.), *Geology and Paleontology of the Shimanto Belt*, Rinyakosaikai Press, Kochi, Japan, pp.179–214.
- Taira, A., 1985: Sedimentary evolution of shikoku subduction zone: The Shimanto Belt and Nankai Trough. In: N. Nasu et al. (eds.), *Formation of Active Ocean Margins*, Terra Scientific Publishing Company (TERRAPUB), Tokyo, pp.835–851.
- Taylor, S.R., 1964: Abundances of chemical elements in the continental crust: a new table. *Geochim. Cosmochim. Acta*, **28**, 1273–1285.
- Yamamoto, K., 1983. Geochemical study of Triassic bedded cherts from Kamiaso, Gifu Prefecture. *J. Geol. Soc. Jpn.*, **89**, 143–162.
- Yamamoto, K., 1987. Geochemical characteristics and depositional environments of cherts and associated rocks in the Franciscan and Shimanto terranes. *Sediment. Geol.*, **52**, 65–108.
- Yamamoto, K. and Sugisaki, R., 1986. Geochemical characteristics of deep-sea sediments around 3-N, 169-W, the Pacific Ocean: samples for GH81-4 cruise, Geological Survey of Japan. *Geol. Surv. Japan Cruise Rept.*, **No. 21**, 195–208.
- Yamamoto, K., Sugisaki, R. and Arai, F., 1986. Chemical aspects of alteration of acidic tuffs and their application to siliceous deposits. *Chem. Geol.*, **55**, 61–76.